Electronic Supplementary Information

Rational design of thermo-responsive adsorbents: demand-oriented active sites for the adsorption of dyes

Yao Jiang, Shu-Feng Shan, Wei Liu, Jing Zhu, Qiu-Xia He, Peng Tan, Lei Cheng, Xiao-Qin Liu and Lin-Bing Sun*

State Key Laboratory of Materials-Oriented Chemical Engineering, Jiangsu National Synergetic Innovation Center for Advanced Materials (SICAM), College of Chemistry and Chemical Engineering, Nanjing Tech University, Nanjing 210009, China. E-mail: lbsun@njtech.edu.cn.

Contents:

• **Methods**

• **Table S1: Textural properties and elemental compositions of samples**

• **Table S2: Physical properties of MS, R@MS, A@MS, and RA@MS**

• **Table S3: The maximum amount of adsorption and desorption of AM on different samples**

• **Figure S1: Schematic synthetic process of the adsorbents**

• **Figure S2: TG curves of the samples**

• **Figure S3: Low-angle XRD patterns of the samples**

• **Figure S4: Wide-angle XRD patterns of the samples**

• **Figure S5: N_2 adsorption-desorption isotherms and pore size distributions of the samples**

• **Figure S6: TEM images of the samples**

• **Figure S7: EDS spectrum of the sample RA@MS**

• **References**

Methods

Chemicals

N-isopropylacrylamide (NIPAM; TCI, 97%) was recrystallized twice from a toluene/hexane solution (v/v = 50:50) and dried under vacuum prior to use. *N*-[3-(dimethylamino) propyl]methacrylamide (DMAPM; TCI, 98%) was purified by passing it through an alumina column and followed by vacuum distillation. azodiisobutyronitrile (AIBN; Sigma-Aldrich, 98%) was recrystallized twice from methanol and dried under reduced pressure before use. Triblock copolymer $EO_{20}PO_{70}EO_{20}$ (P123; Sigma-Aldrich, 99%), tetraethylorthosilicate (TEOS; Sigma-Aldrich, 98%), (3-mercaptopropyl)trimethoxysilane (MPTMS; Sigma-Aldrich), and ethanol (Aladdin, ≥99.9%) were used directly without any further purification. Deionized water was generated by a Milli-Q integral pure and ultrapure water purification system and used in all experiments.

Synthesis of materials

Synthesis of mesoporous silica SBA-15 (MS)

3 g of Pluronic P123 was dissolved in 90 g of aqueous HCl solution (2 M) and 22.5 g distilled water with stirring at 40 °C. After the formation of a homogeneous solution, 6.38 g of silica source TEOS was added and stirred at 40 °C for 24 h, followed by hydrothermal treatment at 100 °C for 24 h in a Teflon-lined autoclave. The as-prepared sample was recovered by filtration, washed with water, and air-dried at room temperature. To remove the surfactant template (P123), 1.0 g of as-prepared sample was refluxed for 48 h in a solution of 200 mL of ethanol followed by washing with deionized water and ethanol extensively. The resulting template-free MS material was placed under high vacuum to remove the remaining solvent in the mesopores.[1-2]

Synthesis of thiol-functionalized MS (SH@MS)

3 g of Pluronic P123 was dissolved in 90 g of aqueous HCl solution (2 M) and 22.5 g distilled water with stirring at 40 °C. After the formation of a homogeneous solution, 5.74 g of silica source TEOS was added and stirred at this temperature for 45 min. Then 0.6 g of MPTMS was added and stirred at 40 °C for 24 h, followed by hydrothermal treatment at 100 °C for 24 h in a Teflon-lined autoclave. The

as-prepared sample was recovered by filtration, washed with water, and air-dried at room temperature. To remove the surfactant template (P123), 1.0 g of as-prepared sample was refluxed for 48 h in a solution of 200 mL of ethanol followed by washing with deionized water and ethanol extensively. The resulting template-free SH@MS material was placed under high vacuum to remove the remaining solvent in the mesopores.

*Synthesis of pNIPAM-functionalized MS (**R**@MS)*

The materials SH@MS (0.3 g) was dispersed in acetone (6 mL), followed by addition of NIPAM (0.2 g) and AIBN (3.0 mg) in a Schlenk tube with a stir bar. After the mixture was sealed and deoxygenated by bubbling argon for 30 min to remove air, the mixture subsequently stirred for 12 h at 0 °C in the dark. Then, the Schlenk tube was placed in an oil bath preheated to 65 °C for 12 h for polymerization. After that, the product was soaked in a large number of acetone for 12 h to remove unreacted monomers and any detachable polymer. The obtained solid was collected by centrifugation and washed with acetone several times and dried under vacuum, leading to the formation of **R**@MS.

*Synthesis of pDMAPM-functionalized MS (**A**@MS)*

The materials SH@MS (0.3 g) was dispersed in acetone (6 mL), followed by addition of DMAPM (0.14 g) and AIBN (3.0 mg) in a Schlenk tube with a stir bar. After the mixture was sealed and deoxygenated by bubbling argon for 30 min to remove air, the mixture subsequently stirred for 12 h at 0 °C in the dark. Then, the Schlenk tube was placed in an oil bath preheated to 65 °C for 12 h for polymerization. After that, the product was soaked in a large number of acetone for 12 h to remove unreacted monomers and any detachable polymer. The obtained solid was collected by centrifugation and washed with acetone several times and dried under vacuum, leading to the formation of **A**@MS.

*Synthesis of pNIPAM and pDMAPM-functionalized MS (**RA**@MS)*

The materials SH@MS (0.3 g) was dispersed in acetone (6 mL), followed by addition of NIPAM (0.2 g), DMAPM (0.14 g) and AIBN (3.0 mg) in a Schlenk tube with a stir bar. After the mixture was sealed and deoxygenated by bubbling argon for 30 min to remove air, the mixture subsequently stirred for 12 h at 0 °C in the dark. Then, the Schlenk tube was placed in an oil bath preheated to 65 °C for 12 h for polymerization. After that, the product was soaked in a large number of acetone for 12 h to remove

unreacted monomers and any detachable polymer. The obtained solid was collected by centrifugation and washed with acetone several times and dried under vacuum, leading to the formation of **RA**@MS.

Characterization

^{13}C cross polarization magic angel spinning NMR (^{13}C CP MAS) spectra were recorded on a Bruker Avance 400 spectrometer (400 MHz). Differential scanning calorimetry (DSC) was performed using a DSC Q100 from TA instruments under nitrogen with 2 ^{o}C min^{-1} ramping rate from 20 to 60 ^{o}C. The DSC curve of the support before polymer modification was also obtained for comparison. The samples were dispersed in deionized water and the resulting slurries were sealed in the sample pans. UV-vis spectra were collected on the SHIMADZU UV-2600 in the region of 200-800 nm.

X-ray diffraction (XRD) patterns of samples were recorded with an X-ray diffractometer (Japan Rigaku D/MAX-γA) using Cu Kα radiation in the 2θ range from 0.6^{o} to 5^{o} and 5^{o} to 80^{o} at 40 kV and 40 mA. Transmission electron microscopy (TEM) and energy-dispersive spectroscopy (EDS) analysis were performed using an FEI Tecnai G2 F30 electron microscope operated at 200 kV. The powder samples were immersed into pure ethanol to make solutions, and a small drop of the solution was transferred onto the top surface of the TEM grids and dried in air. The TEM grids used in this work were 400 mesh Cu grids coated with pure carbon support film (Electron Microscopy Sciences), which were previously glow discharged to make their surfaces hydrophilic. N_2 adsorption-desorption isotherms were measured using ASAP 2020 analyzer at –196 °C. The samples were degassed at 80 °C for 6 h prior to analysis. The Brunauer-Emmett-Teller (BET) surface area was calculated using adsorption data in a relative pressure ranging from 0.05 to 0.3. The total pore volume was determined from the amount adsorbed at a relative pressure of about 0.99. The pore diameter was calculated from the adsorption branch by using the Barrett-Joyner-Halenda (BJH) methods. Fourier transform infrared (IR) spectra of the samples were carried out on a Thermo Scientific Nicolet iS10 spectrometer with KBr wafer technique after diluting the sample with the mass ratio of 100:1 in KBr. The spectra were collected with a 2 cm^{-1} resolution. The elemental analysis (C, H, and N) was performed by a Vario Micro Cube elemental analyzer (Elementar Analysensysteme GmbH, Hanau, Germany). Thermogravimetric (TG) analysis curves were obtained from the use of a thermobalance analyzer (STA-499C, NETZSCH). About 10 mg of sample was heated from room temperature to 800 °C with

a heating rate of 20 °C min^{-1} in a N_2 flow (20 mL·min^{-1}). The amount of grafted polymers was determined by the difference between the weight losses of the materials in the range of 100~800 °C.

Adsorption experiments

Two different guest molecules were used as adsorbates for adsorption study, the acidic molecule (AM) acid orange and the basic molecule (BM) methylene blue. The contents of guest molecules in aqueous solutions were both 20 mg L^{-1}. Adsorption experiments were performed in the quartz cuvette directly in the cell holder of UV-vis spectrophotometer. In a typical adsorption experiment, 2 mg of the adsorbent was weighted precisely and statically dispersed in the aqueous solution (1 mL) water, after 5 min balance with water under 25 or 50 °C, 2 mL containing 25 mg·L^{-1} of guest molecules were added directly. Adsorption was conducted statically at 25 or 50 °C until the equilibrium was reached. The contents of guest molecules in the treated solutions were determined at regular intervals using the UV-vis spectrophotometer.[3-4] The adsorption amount (Q_e) was determined according to formula (1).

$$Q_e = \frac{(c_i - c_e)V}{m} \qquad (1)$$

Where c_i is the initial concentration, c_e is the residual or equilibrium concentration, V is the volume of liquid phase, and m is the mass of adsorbent.

Desorption was carried out by using saturated adsorbents in the mixture of ethanol/water solution at 25 or 50 °C. The dye concentration was measured at appropriate time intervals by UV-vis spectrophotometer and the desorption amount (Q_d) was determined according to formula (2).

$$Q_d = \frac{c_d V}{m Q_e} \times 100\% \qquad (2)$$

Where c_d is desorption equilibrium concentration.

Desorption curves of sample for the response subjected to periodically switching (dynamic desorption) during desorption measurements were carried out by change of temperature every 20 min between 25 and 50 °C.

Additional Result and Discussion

Structural parameters can be obtained from XRD patterns at small angle range. The (100) interplanar spacing (d_{100}) is calculated from the Bragg's law ($2d\sin\theta=n\lambda$) and shown in Table S2. The unit cell parameter a_0 (corresponding to the distance between the pores) can be calculated by $a_0=2d_{100}/\sqrt{3}$. The pore wall thickness (D_w) of samples is thus obtained from the equation $D_w=a_0-D_p$, where D_p is the pore diameter.[5] As shown in Figure S3 and Table S2, in accord with the shift of peaks to higher angles, a slight decrease of the unit cell parameter is observed for all the composite materials (**R**@MS, **A**@MS, and **RA**@MS). Moreover, a decrease of pore diameter and an increase of the wall thickness is observed after incorporating the polymers, indicating the location of polymers in the pores. The pore size from N_2 adsorption can be compared with that from TEM. Taking **RA**@MS as an example, the pore size is 4.6 nm from N_2 adsorption, which is in agreement with that from TEM (4.9 nm).

The low-angle X-ray diffraction (XRD) patterns of **R**@MS, **A**@MS, and **RA**@MS are in agreement with a 2D hexagonal pore regularity *p*6*mm* space group (Fig. S3).[6] Also they are in good consistent with the sample of MS, suggesting that the ordered mesostructure is well maintained after incorporating **R** and/or **A** polymers. A single broad diffraction peak at about 23° is observed in the wide-angle XRD pattern of MS, which can be ascribed to amorphous silica walls (Fig. S4).[7] New diffraction peaks were not observed after the introduction of **R** and/or **A** polymers.[8]

The LCST phenomenon of **R**@MS can be explained by the interaction of hydrogen bonding between **R** and surrounding water molecules. When the temperature is below LCST, it is favorable for the hydrogen bonding interaction between the **R** and surrounding water molecules, resulting in the stretching conformation of polymers. With increasing temperature, intramolecular hydrogen bonding between C=O and N–H groups among the **R** chains gives a compact and shrinking conformation.[9-10] In consideration of the polymers in the pores of MS and the active sites in the chain of polymers, the active sites might be reversibly blocked and exposed by the change of temperature. This feature makes our material useful in the process of adsorptive separation.

On the basis of the dyes adsorption results, thermo-responsive polymers **R** and active sites **A** assist the adsorbent to achieve selective adsorption and high-efficiency regeneration. It is noteworthy that quite a narrow temperature difference between 25 and 50 °C, is enough to acquire the high-efficiency adsorption performance. And it turns out that the application of **RA**@MS in TSA process, merely a small temperature difference is required, also means that the smart adsorbent consumes much less

energy compared with conventional adsorbents. Such unusual adsorption behavior is caused by the cooperation between thermo-responsive feature and active sites. However, conventional adsorbents with fixed active sites are unlikely to realize this adsorption performance.

Table S1 Textural properties and elemental compositions of samples

Sample	S_{BET} (m^2 g^{-1})	V_p (cm^3 g^{-1})	D_p (nm)	Elemental analysis (wt %)		
				C	H	N
MS	845	1.17	8.4	0.67	0.83	0.02
SH@MS	697	0.82	6.5	12.14	3.41	0.08
R@MS	294	0.40	5.2	20.31	3.78	2.97
A@MS	241	0.34	5.0	15.47	3.86	1.42
RA@MS	158	0.31	4.6	29.44	5.76	5.28

Table S2 Physical properties of MS, **R**@MS, **A**@MS, and **RA**@MS

Sample	d_{100}[a] (nm)	a_0[b] (nm)	D_p[c] (nm)	D_w[d] (nm)
MS	10.3	11.9	8.4	3.5
R@MS	9.7	11.2	5.2	6.0
A@MS	9.8	11.3	5.0	6.3
RA@MS	9.5	11.0	4.6	6.4

[a] The plane distance d_{100} was computed according to the Bragg's law ($n\lambda=2d\sin\theta$).

[b] The unit cell parameter was calculated as $a_0=2d_{100}/\sqrt{3}$ and corresponds to the distance between the pores.

[c] The pore diameters calculated through the BJH method.

[d] The wall thickness was calculated as $D_w=a_0-D_p$.

Table S3 The maximum amount of adsorption (Ads_{max}) and desorption (Des_{max}) of AM on **A**@MS, **R**@MS, and **RA**@MS at 25 and 50 °C

Sample	T (°C)	Ads_{max} (mg g^{-1})	Des_{max} (mg g^{-1})
A@MS	25	12.8	2.0
	50	10.6	5.6
R@MS	25	0.3	<0.1
	50	0.1	0.1
RA@MS	25	21.2	3.1
	50	7.7	20.8

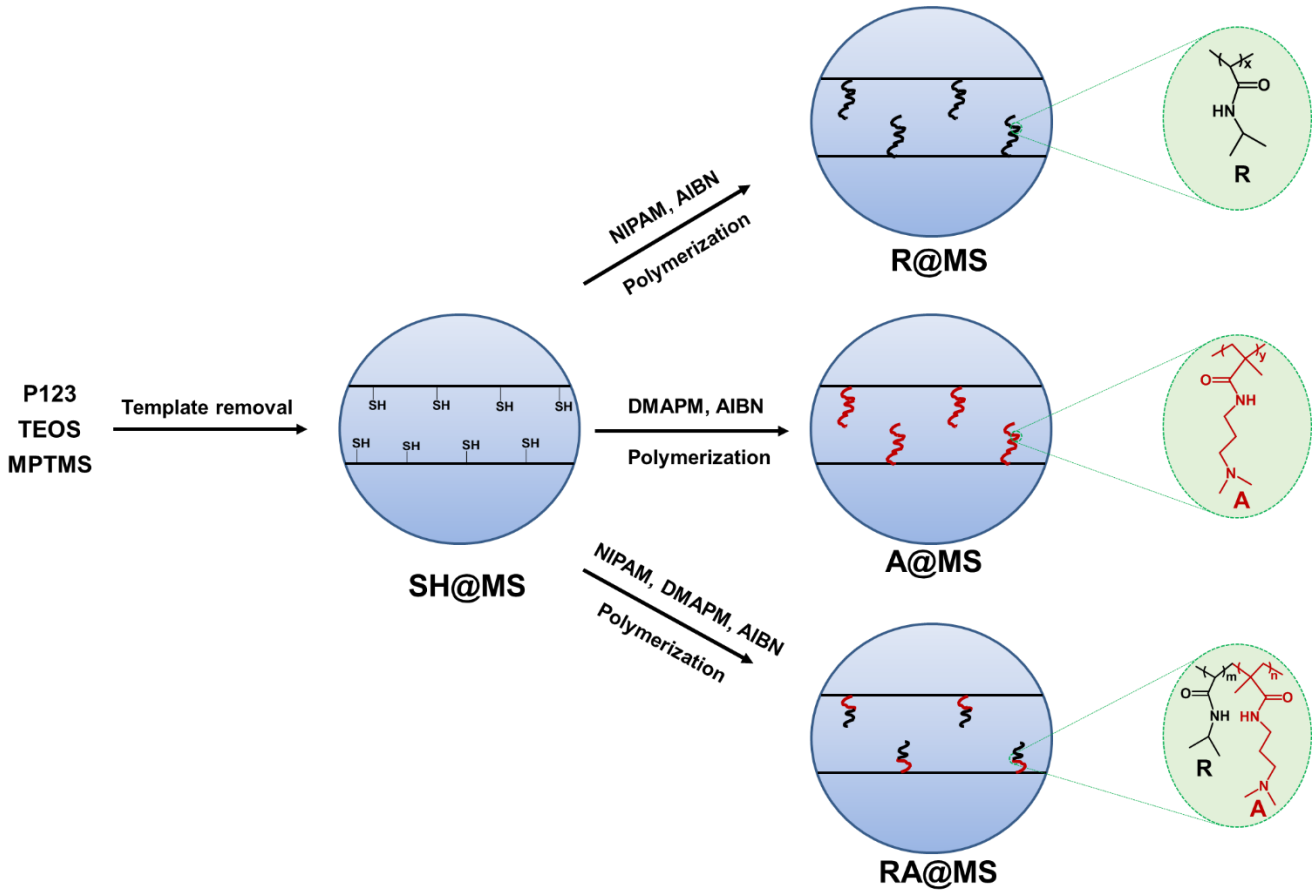

Figure S1. Schematic synthetic process of the adsorbents **R**@MS, **A**@MS, and **RA**@MS.

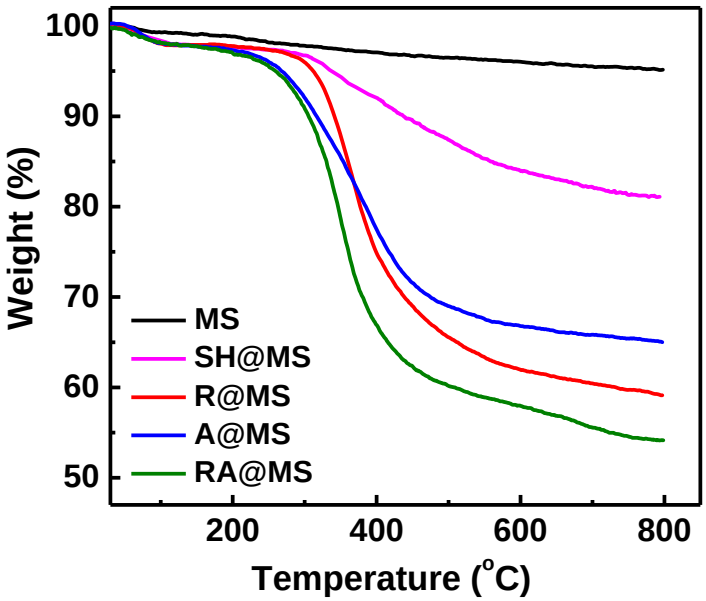

Figure S2. TG curves of the samples MS, SH@MS, **R**@MS, **A**@MS, and **RA**@MS. TG analysis shows that 24.2 wt% (**R**@MS), 12.8 wt% (**A**@MS), and 28.6 wt% (**RA**@MS) of polymers are introduced respectively. For the sample of **RA**@MS, the contents of **R** and **A** are about 17.4 and 11.2 wt%, respectively.

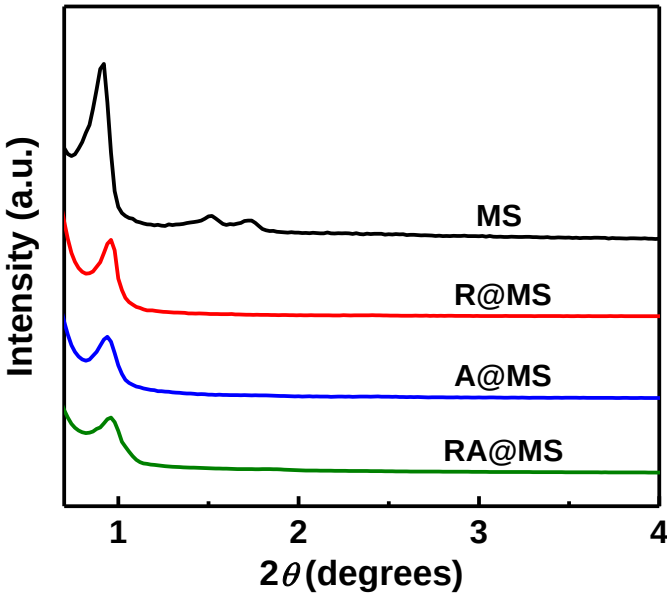

Figure S3. Low-angle XRD patterns of the samples MS, **R**@MS, **A**@MS, and **RA**@MS.

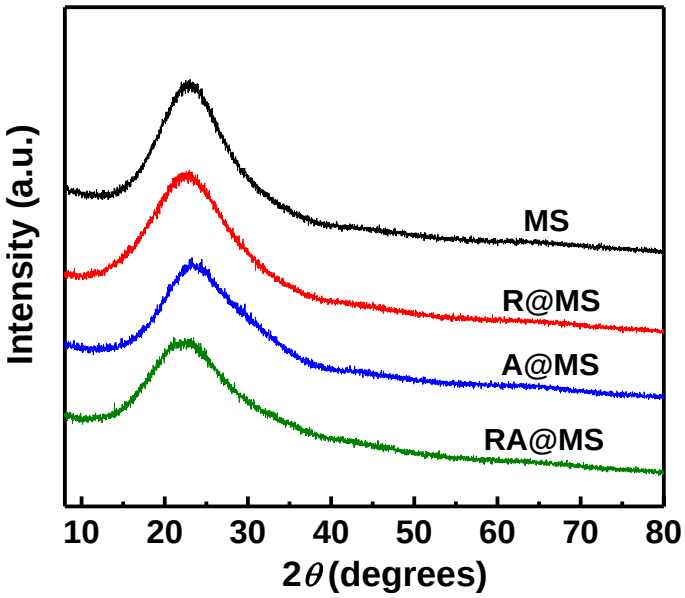

Figure S4. Wide-angle XRD patterns of the samples MS, **R**@MS, **A**@MS, and **RA**@MS.

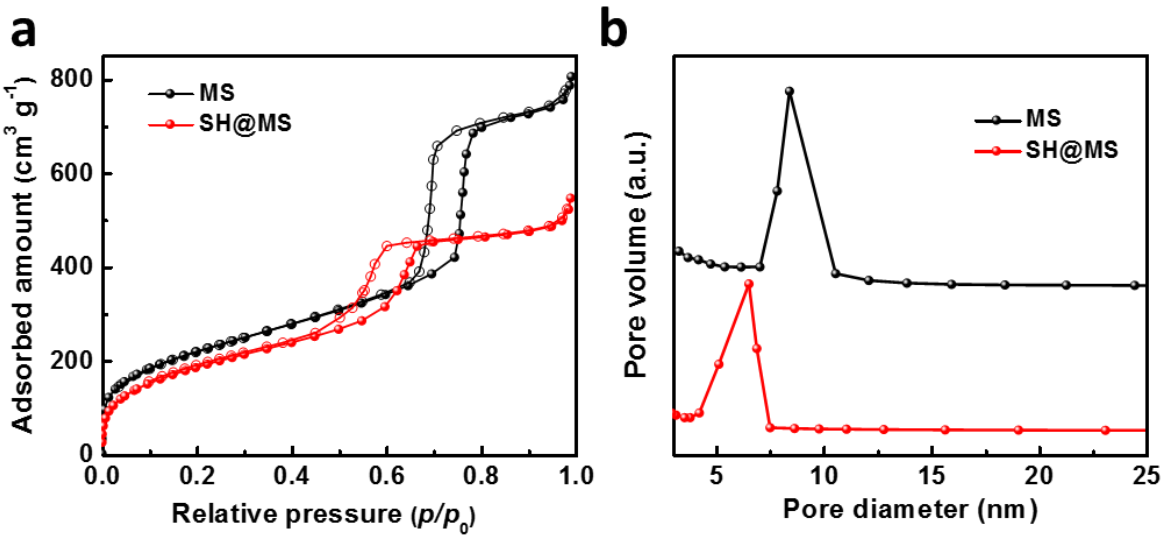

Figure S5. (a) N_2 adsorption-desorption isotherms, (b) pore size distributions of the samples MS and SH@MS.

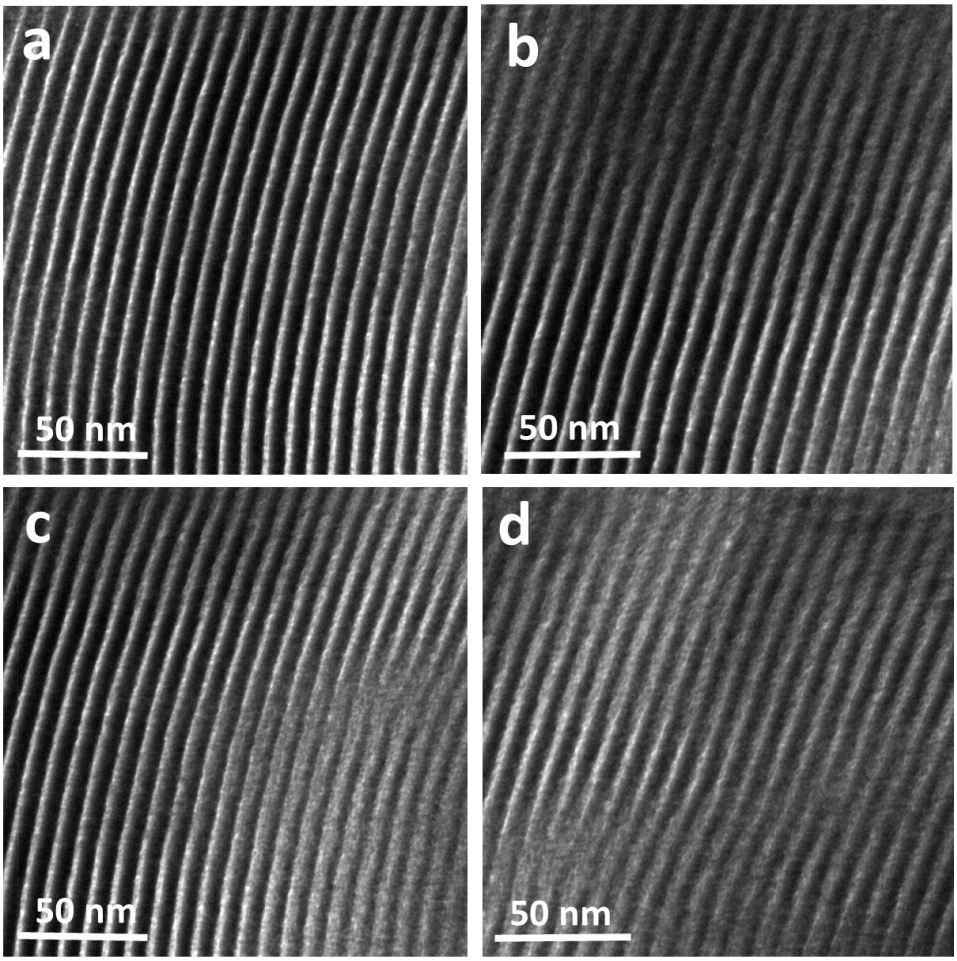

Figure S6. TEM images of the samples (a) MS, (b) **R**@MS, (c) **A**@MS, and (d) **RA**@MS.

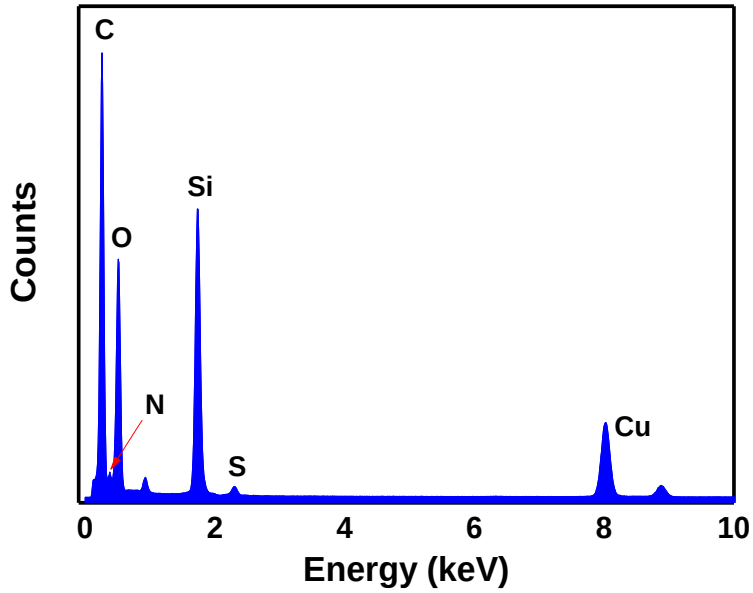

Figure S7. EDS spectrum of the sample **RA**@MS. The element Cu was originated from the Cu grid used in the measurement.

References

S1 D. Zhao, J. Feng, Q. Huo, N. Melosh, G. H. Fredrickson, B. F. Chmelka and G. D. Stucky, *Science*, 1998, **279**, 548.

S2 L.-B. Sun, J.-R. Li, W. Lu, Z.-Y. Gu, Z. Luo and H.-C. Zhou, *J. Am. Chem. Soc.*, 2012, **134**, 15923.

S3 K. Y. Ho, G. McKay and K. L. Yeung, *Langmuir*, 2003, **19**, 3019.

S4 X. Zhuang, Y. Wan, C. Feng, Y. Shen and D. Zhao, *Chem. Mater.*, 2009, **21**, 706.

S5 A. Venezia, G. Di Carlo, L. Liotta, G. Pantaleo and M. Kantcheva, *Appl. Catal., B*, 2011, **106**, 529.

S6 Y. Jiang, P. Tan, Y.-H. Kang, Z.-M. Xing, L. Cheng, L. Zhu, X.-Q. Liu and L.-B. Sun, *Adv. Mater. Interfaces*, 2016, **3**, 1500829.

S7 L. Cheng, Y. Jiang, N. Yan, S. F. Shan, X. Q. Liu and L. B. Sun, *ACS Appl. Mater. Interfaces*, 2016, **8**, 23404.

S8 Y. Jiang, P. Tan, L. Cheng, S.-F. Shan, X.-Q. Liu and L.-B. Sun, *Phys. Chem. Chem. Phys.*, 2016, **18**, 9883.

S9 A. Halperin, M. Kröger and F. M. Winnik, *Angew. Chem., Int. Ed.*, 2015, **54**, 15342.

S10 H. Zhang and A. I. Cooper, *Adv. Mater.*, 2007, **19**, 2439.